

The magnetization behavior and magnetic viscosity of $\text{Sm}(\text{Co}, \text{Fe}, \text{Cu}, \text{Zr})_z$ ribbons with different temperature dependence of coercivity

Jinzi Wang,¹ Renjie Chen,^{2,a)} Chuanbing Rong,³ Zhuang Liu,² Hongwei Zhang,⁴ Baogen Shen,⁴ and Aru Yan²

¹Ningbo University of Technology, Ningbo 315211, People's Republic of China and Ningbo Institute of Materials Technology and Engineering, Chinese Academy of Sciences, Ningbo 315201, People's Republic of China

²Zhejiang Province Key Laboratory of Magnetic Materials and Application Technology, Ningbo Institute of Materials Technology and Engineering, Chinese Academy of Sciences, Ningbo 315201, People's Republic of China

³Department of Physics, University of Texas at Arlington, Arlington, Texas 76019, USA

⁴State Key Laboratory of Magnetism, Institute of Physics and Centre for Condensed Matter Physics, Chinese Academy of Sciences, Beijing 100080, People's Republic of China

(Presented 19 January 2010; received 17 October 2009; accepted 15 December 2009; published online 15 April 2010)

Two types of $\text{Sm}(\text{Co}, \text{Fe}, \text{Cu}, \text{Zr})_z$ ribbons with different temperature dependence of coercivity are investigated in comparison at different temperatures. It is found that their magnetization behaviors and magnetic viscosity are distinctly different. The magnetization of sample A (with abnormal temperature dependence of coercivity) behaves as a single phase permanent magnet at room temperature, and then becomes similar to a nanocomposite magnet with the increase of temperature. However, sample B (with negative temperature coefficient of coercivity) is similar to a nanocomposite magnet at the whole temperature range. The magnetic viscosity is mainly determined by the irreversible magnetization for both ribbons, while there emerges an extra small peak of magnetic viscosity coefficient $S(H)$ at low field and high temperature for sample B. The different content and distribution of Cu in the cell boundary phase are proposed to be responsible for the differences of temperature dependence of coercivity, magnetization, and magnetic viscosity behaviors of these two types of $\text{Sm}(\text{Co}, \text{Fe}, \text{Cu}, \text{Zr})_z$ ribbons. © 2010 American Institute of Physics. [doi:10.1063/1.3334540]

$\text{Sm}(\text{Co}, \text{Fe}, \text{Cu}, \text{Zr})_z$ permanent magnets (PMs), with a complex cellular microstructure consisting of 2:17 type cells surrounded by a Cu-rich 1:5 cell boundary phase, have been always the ideal candidates for high-temperature magnetic applications because of their excellent permanent magnetic properties at high temperatures.¹⁻³ Since the 1990s, the $\text{Sm}(\text{Co}, \text{Fe}, \text{Cu}, \text{Zr})_z$ PMs have attracted intensive attention again because of the observed abnormal temperature dependence of coercivity.⁴ Due to the complexity of microstructure and element distribution, the physics of magnetization in $\text{Sm}(\text{Co}, \text{Fe}, \text{Cu}, \text{Zr})_z$ has been controversial. However, it is generally accepted that it is closely related to the characteristics of the cell boundary phase.^{2,4-6} In our previous study, we have found that the Cu content in the boundary phase determines the intensity of the intergrain exchange coupling (IGEC) in $\text{Sm}(\text{Co}, \text{Fe}, \text{Cu}, \text{Zr})_z$ ribbons.⁷ In this paper, the magnetization behaviors and magnetic viscosity are studied to provide a further comprehension on the temperature dependence of magnetization mechanism in $\text{Sm}(\text{Co}, \text{Fe}, \text{Cu}, \text{Zr})_z$ PMs.

The ribbons of $\text{Sm}(\text{Co}_{\text{bal}}\text{Fe}_{0.1}\text{Cu}_{0.1}\text{Zr}_{0.03})_{7.0}$ (sample A) and $\text{Sm}(\text{Co}_{\text{bal}}\text{Fe}_{0.1}\text{Cu}_{0.1}\text{Zr}_{0.03})_{7.5}$ (sample B) were prepared by a melt-spinning technique and a subsequent heat treatment. The detailed experimental process was given in Ref. 7. The

magnetization behaviors were studied using the DC demagnetization (DCD) method,^{8,9} and the schematic illustration of measurements is shown in Fig. 1. The magnetic properties were investigated by a high temperature vibrating sample magnetometer (LakeShore 7410, maximum field 24 kOe). The measurements were performed along the longitudinal direction of ribbons and no demagnetization correction was done. The test time for investigations of magnetic viscosity was 100 s.

The experimental results indicate that the abnormal and normal temperature dependences of coercivity are obtained in samples A and B, respectively.⁷ Figures 2(a) and 2(b) give the major demagnetization curves and recoils loops at room

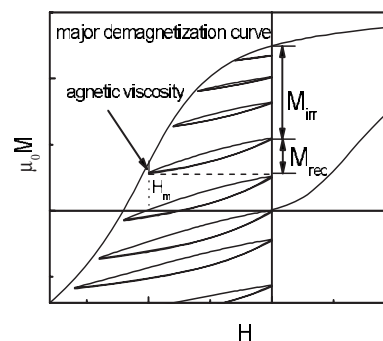


FIG. 1. Schematic illustration of magnetic measurements.

^{a)}Electronic mail: chenrj@nimte.ac.cn.

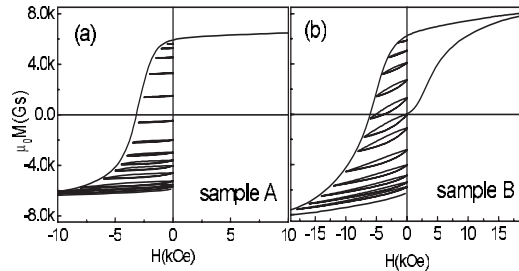
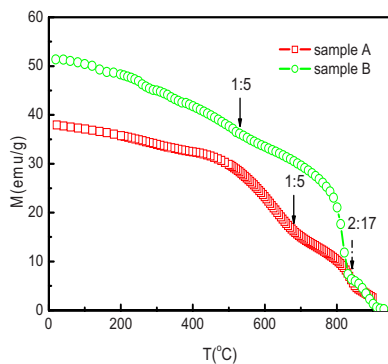
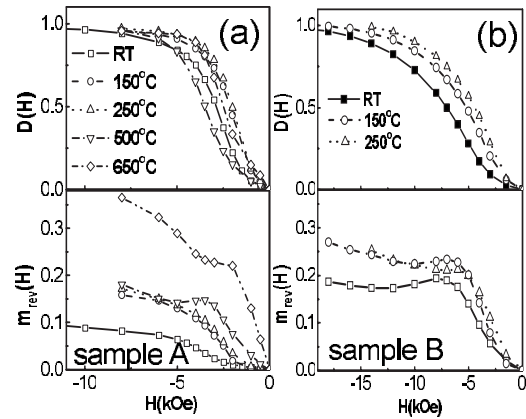


FIG. 2. Major demagnetization curves and recoil loops.

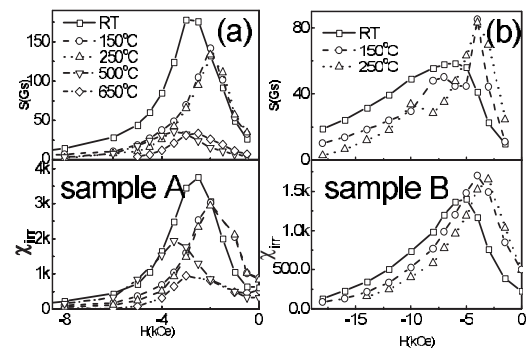
temperature (RT). It can be seen that the magnetization in sample A is almost irreversible, which contrasts significantly with that in sample B. Many experimental results indicate that the magnets of $\text{Sm}(\text{Co}, \text{Fe}, \text{Cu}, \text{Zr})_z$ with different temperature dependence of coercivity possess the same microstructure.^{3,8} And the coercivity dependence on temperature is closely related to the Cu content in the cell boundary phase.^{3,8,9} Considering the larger ratio z and the Cu concentration at the cell boundaries, there is a relatively smaller content of 1:5 phase with a higher content of Cu in sample B (see our previous work in Ref. 7).⁵ Therefore, the T_C (1:5) can be used to characterize the Cu content of the cell boundary phase.¹⁰ To verify this expectation, the temperature dependences of magnetization of the two samples are analyzed, as shown in Fig. 3. One can find that T_C (2:17) is almost constant but T_C (1:5) is quite different, ~ 645 and 505 °C for samples A and B, respectively. This indicates that the Cu content in the cell boundary phase of sample B is higher than that of sample A. Therefore, the boundary phase in sample B is magnetically softer, which results in its magnetization behaviors similar to nanocomposite PMs.

Figure 4 shows the reversible and irreversible magnetization [$m_{\text{rev}}(H)$ and $D(H)$] at different temperatures. The $m_{\text{rev}}(H)$ for sample B is higher than that for sample A due to a stronger exchange-spring interaction. Moreover, the maxima of $m_{\text{rev}}(H)$ are obtained in the vicinity of H_{ci} for sample B, which is similar to that found in nanocomposite PMs.^{11–14} It is resulted from the competition between the external field and IGEC. At high temperatures (>500 °C), the $m_{\text{rev}}-H$ curves of sample A are similar to those of sample B. However, at lower temperatures, the $m_{\text{rev}}(H)$ value of sample A increases monotonously with the increase of external field. The cell boundary phase of sample A is magnetically

FIG. 3. (Color online) Temperature dependences of magnetization M .FIG. 4. Reversible magnetization $m_{\text{rev}}(H)$ and irreversible magnetization $D(H)$ at different temperatures.

ically harder at low temperatures, due to the relatively less content of Cu. With temperature increasing, it starts softening, which makes the field dependence of m_{rev} similar to that of sample B and nanocomposite PMs. The field at the derivative $dD(H)/dH$ peak corresponds to the reversal field H_n of irreversible magnetization, and the full width at half height suggests the H_n distribution of grains in magnets. According to Fig. 4, the H_n distribution of sample A is obviously narrower than that of sample B. This indicates that the distribution of magnetic intrinsic properties of sample A is more homogeneous than that of sample B. The magnitudes of H_n for samples A and B at RT are 2.6 and 5.4 kOe, respectively, which are slightly lower than their coercivities. Moreover, the temperature dependences of H_n are similar to those of H_{ci} .

The magnetic viscosity coefficient S is obtained from the time dependent magnetization databased on the relation $M(t) = M_0 - S \ln(t + t_0)$. Figure 5 shows S and the irreversible susceptibility χ_{irr} as functions of external field. It is found that the field dependences of S and χ_{irr} are quite similar for both samples, which indicates that the magnetic viscosity is mainly determined by the irreversible magnetization. However, the values of S and χ_{irr} of sample A are much higher than those of sample B. According to the study of Feutrill et al.,¹² the S value of a two-phase material is smaller than that of a single phase material because of the absence of magnetic relaxation in the soft phase. As for sample B, the “soft” 1:5 cell boundary phase makes the magnetic viscosity behave

FIG. 5. Field dependences of magnetic viscosity coefficient $S(H)$ and irreversible susceptibility χ_{irr} at different temperatures.

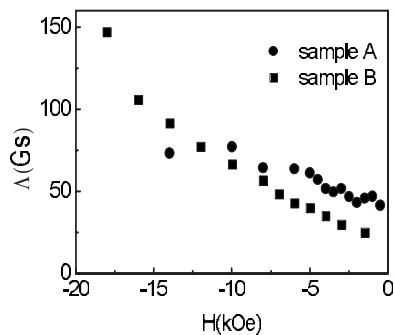


FIG. 6. Field dependence of fluctuation field Λ at RT.

like a two-phase magnet. Otherwise, the magnetic viscosity is determined by the distribution $f(E)$ of thermal activation energies and there is a relationship $S \propto f(E)$. As shown in Fig. 5, the sharper S peak in sample A at RT suggests that there is a narrower distribution of thermal activation energy than in sample B. It might be resulted from the homogeneity difference of magnetic properties between sample A and B. The same reason results in a stronger domain wall pinning and a higher coercivity for sample B at RT. With increasing temperature, the $S(H)$ peak position of sample A exhibits a non-monotonous temperature dependence, which is similar to the temperature dependence of coercivity and is possibly due to the distribution change of thermal activation energy by IGEC. It is interesting that an extra small $S(H)$ peak emerges at low field and high temperature in sample B. It is possibly due to the different responding rates of thermal activation energy for the cell and cell boundary phases against the temperature variation.

The fluctuation field Λ can be expressed as $\Lambda = S/\chi_{\text{irr}} = k_B T/vM_S$,¹⁵ where v is the activation volume of the magnetic relaxation process. Figure 6 gives the field dependences of Λ for sample A and B at RT. According to the research results of El-Hilo *et al.*¹⁶ and Crew *et al.*,¹⁷ Λ increases linearly with increasing external field in a system of isotropic Stoner–Wohlfarth particles. Although the ribbons are magnetically isotropic in our work, the IGEC makes the relation between Λ and H deviate from linearity. This is particularly

significant in sample A due to a stronger IGEC. The activation volume v decreases with increasing field, which is similar to the results of $\text{Sm}_2\text{Fe}_{14}\text{Ga}_3\text{C}_2/\alpha\text{-Fe}$ system.¹² Moreover, v of sample B is larger than that of sample A at RT. As mentioned above, the magnetic crystalline anisotropy of the cell boundary phase in sample B is weaker than that in sample A, and thus the irreversible magnetization occurs easily, which therefore results in a larger activation volume.

The authors grateful acknowledge the supports of the Natural Science Foundation of Zhejiang (Grant Nos. Y407174 and Y4090583), the Major Scientific and Technological Special of Zhejiang (Grant No. 2007C11046), and the National Basic Research Program of China (Grant No. 2010CB934601).

¹G. C. Hadjipanayis, *J. Magn. Magn. Mater.* **200**, 373 (1999).

²D. Goll, I. Kleinschroth, W. Sigle, and H. Kronmüller, *Appl. Phys. Lett.* **76**, 1054 (2000).

³S. Liu, J. Yang, G. Doyle, G. Potts, and G. E. Kuhl, *J. Appl. Phys.* **87**, 672 (2000).

⁴A. G. Popov, A. V. Korolev, and N. N. Shchegoleva, *Phys. Met. Metallogr.* **60**, 100 (1990).

⁵G. C. Hadjipanayis, W. Tang, Y. Zhang, S. T. Chui, J. F. Liu, C. Chen, and H. Kronmüller, *IEEE Trans. Magn.* **36**, 3382 (2000).

⁶A. M. Gabay, W. Tang, Y. Zhang, and G. C. Hadjipanayis, *Appl. Phys. Lett.* **78**, 1595 (2001).

⁷R. J. Chen, J. Z. Wang, H. W. Zhang, B. G. Shen, and A. Yan, *J. Phys. D: Appl. Phys.* **40**, 4391 (2007).

⁸J. F. Liu, T. Chui, D. Dimitrov, and G. C. Hadjipanayis, *Appl. Phys. Lett.* **73**, 3007 (1998).

⁹J. F. Liu, Y. Zhang, D. Dimitrov, and G. Thomas, *J. Appl. Phys.* **85**, 2800 (1999).

¹⁰J. Zhang, H. Liu, C. B. Rong, H. W. Zhang, S. Y. Zhang, B. G. Shen, Y. Q. Bai, and B. H. Li, *Appl. Phys. Lett.* **83**, 1172 (2003).

¹¹E. F. Kneller and R. Hawig, *IEEE Trans. Magn.* **27**, 3588 (1991).

¹²E. H. Feutrill, P. G. McCormick, and R. Street, *J. Phys. D: Appl. Phys.* **29**, 2320 (1996).

¹³H. W. Zhang, W. Y. Zhang, A. R. Yan, and B. G. Shen, *Acta Phys. Sin.* **48**, S211 (1999).

¹⁴H. W. Zhang, S. Y. Zhang, B. G. Shen, D. Goll, and H. Kronmüller, *Chin. Phys.* **10**, 1169 (2001).

¹⁵P. Gaunt, *J. Appl. Phys.* **59**, 4129 (1986).

¹⁶M. El-Hilo, K. O'Grady, H. Pferffer, R. W. Chantrell, and R. J. Veitch, *IEEE Trans. Magn.* **28**, 2689 (1992).

¹⁷D. C. Crew, S. H. Farrant, P. G. McCormick, and R. Street, *J. Magn. Magn. Mater.* **163**, 299 (1996).